Acta Oceanol. Sin., 2021, Vol. 40, No. 9, P. 94–104
https://doi.org/10.1007/s13131-021-1897-9
http://www.aosocean.com
E-mail: ocean2@hyxb.org.cn

Simultaneous nitrification and denitrification conducted by *Halomonas venusta* MA-ZP17-13 under low temperature conditions

Guizhen Li[1, 2, 3, 4], Qiliang Lai[2, 3, 4], Guangshan Wei[2, 3, 4, 5], Peisheng Yan[1], Zongze Shao[1, 2, 3, 4, 5*]

[1] School of Environment, Harbin Institute of Technology, Harbin 150090, China

[2] Key Laboratory of Marine Genetic Resources, Third Institute of Oceanography, Ministry of Natural Resources, Xiamen 361005, China

[3] State Key Laboratory Breeding Base of Marine Genetic Resources, Xiamen 361005, China

[4] Fujian Key Laboratory of Marine Genetic Resources, Xiamen 361005, China

[5] Sourthern Marine Science and Engineering Guangdong Laboratory (Zhuhai), Zhuhai 519080, China

Received 23 October 2020; accepted 19 February 2021

Abstract

Nitrification is a key step in the global nitrogen cycle. Compared with autotrophic nitrification, heterotrophic nitrification remains poorly understood. In this study, *Halomonas venusta* MA-ZP17-13, isolated from seawater in shrimp aquaculture (*Penaeus vannamei*), could simultaneously undertake nitrification and denitrification. With the initial ammonium concentration at 100 mg/L, the maximum ammonium-nitrogen removal rate reached 98.7% under the optimal conditions including C/N concentration ratio at 5.95, pH at 8.93, and NaCl at 2.33%. The corresponding average removal rate was 1.37 mg/(L·h) (according to nitrogen) in 3 d at 11.2°C. By whole genome sequencing and analysis, nitrification- and denitrification-related genes were identified, including ammonia monooxygenase, nitrate reductase, nitrite reductase, nitric oxide dioxygenase and nitric oxide synthase; while no gene encoding hydroxylamine oxidase was identified, it implied the existence of a novel nitrification pathway from hydroxylamine to nitrate. These results indicate heterotrophic bacterium *H. venusta* MA-ZP17-13 can undertake simultaneous nitrification and denitrification at low temperature and has potential for NH_4^+-N/NH_3-N removal in marine aquaculture systems.

Key words: *Halomonas*, heterotrophic nitrification, denitrification, ammonia oxidization, ammonia removal

Citation: Li Guizhen, Lai Qiliang, Wei Guangshan, Yan Peisheng, Shao Zongze. 2021. Simultaneous nitrification and denitrification conducted by *Halomonas venusta* MA-ZP17-13 under low temperature conditions. Acta Oceanologica Sinica, 40(9): 94–104, doi: 10.1007/s13131-021-1897-9

1 Introduction

Nitrogen (N) compounds are indispensable in biological metabolic processes and play vital roles in nutrient cycling. Inorganic ammonium (NH_4^+) is generally considered an undesirable product because it can cause water quality problems and has a pungent smell (He et al., 2017). Water quality is crucial to the aquaculture industry, and the concentration of NH_4^+-N/NH_3-N is an important indicator of water quality in aquaculture. Many N-containing organic compounds can be excreted under high feed loading rate of aquaculture organisms, which can generate a large number of harmful N-containing substances such as NH_3 and nitrite (NO_2^-), causing acute poisoning of aquaculture organisms (Shan and Obbard, 2001; Lin and Chen, 2003). High concentrations of NH_3 in aquaculture water will affect the cell membrane and enzymatic activity of aquaculture organisms, and even destroy the excretory system and osmotic balance in serious cases (Atanassov et al., 1994). NH_3-N in water is composed of two forms: ionized ammonia (or ammonium: NH_4^+-N) and unionized ammonia (NH_3-N) (Armstrong et al., 1978; Thurston et al., 1981). Compared with NH_4^+-N, NH_3-N is more toxic, because the neutral charge and small size of the molecule that can easily pass through cell membrane (Smart, 1978). It was reported that the 48 h lethal concentration (LC_{50}) values for NH_3-N to *Litopenaeus vannamei* were 2.09 mg/L to 2.26 mg/L in shrimp aquaculture (Schuler et al., 2010). Therefore, controlling the NH_3-N concentration in aquaculture water is particularly important.

Generally, the treatment of NH_4^+-N/NH_3-N is mainly carried out by physical and biological methods in aquaculture. The main physical method is to regularly sprinkle zeolite powder or Maifan stone into the water (Wei et al., 2010; Kan et al., 2011), but this approach is a palliative rather than a cure; the most common and cost-effective method for NH_4^+-N/NH_3-N removal is biological treatment, which involves a combined process of autotrophic nitrification and heterotrophic denitrification (Kim et al., 2005; Chiu et al., 2007; Zhu et al., 2008; Zhao et al., 2010a; Huang et al., 2013). However, this conventional method tends to be time-consuming due to the low rate of nitrification and the separation of aerobic and anoxic phases (Zhu et al., 2008; Huang et al., 2013).

Foundation item: The COMRA Program under contract No. DY135-B2-01; the Xiamen Ocean Economic Innovation and Development Demonstration Project under contract No. 16PZP001SF16; the National Infrastructure of Natural Resources for Science and Technology Program of China under contract No. NIMR-2017-9.
*Corresponding author, E-mail: shaozz@163.com

In recent years, bacteria capacity of simultaneous nitrification and denitrification (SND) have been identified from various environments (Hooper et al., 1997). Many bacteria capacity of SND have been studied from biological N removal systems (Zhao et al., 2010a; Yao et al., 2013; Ren et al., 2014; He et al., 2016; Yu et al., 2016). However, most of these nitrifying strains were mainly carried out under mesophilic conditions (around 30°C) (Zhao et al., 2010b; Chen and Ni, 2012; Huang et al., 2013). Nitrification was strongly inhibited at temperatures below 10°C (Carrera et al., 2003; Rodriguez-Caballero et al., 2012; Huang et al., 2013). Therefore, NH_4^+-N/NH_3-N removal at low temperature remains an unresolved problem.

To obtain bacteria that are capable of effective NH_4^+-N/NH_3-N removal at low temperature, bacteria were enriched and isolated from surface seawater of a higher-place pond of *Penaeus vannamei*. Among the obtained isolates, *Halomonas venusta* MA-ZP17-13 showed high efficiency in removing NH_4^+-N/NH_3-N with no accumulation of NO_2^--N at 10°C. Moreover, it was also capable for heterotrophic nitrification and aerobic denitrification. The aims of this study are (1) to obtain bacteria that are capable for effective NH_4^+-N/NH_3-N removal at low temperature; (2) to study the characteristics of NH_4^+-N/NH_3-N removal of starin MA-ZP17-13 at low temperature. Studies indicate strain MA-ZP17-13 has a great potential in NH_4^+-N/NH_3-N removal from aquaculture water at low temperature.

2 Materials and methods

2.1 *Sampling and strain isolation*

Surface seawater of higher-place *P. vannamei* ponds was sampled in June 2018. The aquaculture seawater sample (24.02°N, 117.83°E) was obtained from an aquaculture farm in Zhangpu County, Zhangzhou City, Fujian Province, China. The seawater was diluted and spread on heterotrophic nitrification medium (HNM) (Xu et al., 2017). After 4 d of aerobic incubation at 28°C, single colonies were picked. Purity was confirmed by the uniformity of cell morphology after repeated streaking. During bacterial screening process, a strain named MA-ZP17-13 was isolated along with many other bacterial isolates. For morphological and biochemical characterization, strain MA-ZP17-13 was cultivated on marine agar 2216 medium. For long-time storage, the strain was suspended in 20.0% glycerol solution at –80°C and deposited in Marine Culture Collection of China under accession number MCCC 1A14584.

2.2 *Culture media*

Marine agar 2216 medium (BD Difco) (Li et al., 2019) contained (per L): 5.0 g peptone, 1.0 g yeast extract, 0.1 g $FeC_6H_5O_7$, 19.45 g NaCl, 8.8 g $MgCl_2$, 3.24 g Na_2SO_4, 1.8 g $CaCl_2$, 0.55 g KCl, 0.16 g $NaHCO_3$, 0.08 g KBr, 34.0 mg $SrCl_2$, 22.0 mg H_3BO_3, 4.0 mg Na_2SiO_3, 2.4 mg NaF, 1.6 mg NH_4NO_3, 8.0 mg Na_2HPO_4.

HNM (pH=7.2) (Xu et al., 2017) contained (per L): 0.24 g $(NH_4)_2SO_4$, 1.12 g $C_4H_4Na_2O_4{\cdot}6H_2O$, 0.05 g $MgSO_4{\cdot}7H_2O$, 0.5 g KH_2PO_4, 2.5 g K_2HPO_4, 30 g NaCl, 0.05 g $MnSO_4$, 0.05 g $FeSO_4$ and 1 mL trace element solution. HNM medium (inorganic medium) was used to determine the NH_4^+-N removal ability of the isolate strain.

Denitrification medium (DM; pH = 7.2) (Xu et al., 2017) contained (per L) : 1.08 g KNO_3, 8.43 g $C_4H_4Na_2O_4{\cdot}6H_2O$, 7.9 g $Na_2HPO_4{\cdot}7H_2O$, 1.5 g KH_2PO_4, 0.1 g $MgSO_4{\cdot}7H_2O$, 30 g NaCl, 1 mL trace element solution. The isolate was cultivated in DM medium to test the ability of denitrification.

Trace element solution contained (per L): 2 mg $CaCl_2$, 50 mg $FeCl_3{\cdot}6H_2O$, 0.5 mg $CuSO_4$, 0.5 mg $MnCl_2{\cdot}4H_2O$ and 10 mg $ZnSO_4{\cdot}7H_2O$. Cultures were incubated at 10°C and spun at 150 r/min, unless noted otherwise.

2.3 *Estimation the N removal and conversion capacity of strain MA-ZP17-13*

The strain MA-ZP17-13 was activated on marine agar 2216 plates, and inoculated into 100 mL marine broth 2216 medium and cultured at 150 r/min and 10°C for 24 h. The culture of 2 mL was centrifuged to remove the medium and washed twice with sterilized seawater, then inoculated into 100 mL HNM medium for ammonia removal tests. After incubated at 10°C and 150 r/min for 15 h under aerobic conditions, 5 mL liquid cultures were sampled serially at intervals of several hours to detect the concentrations of NH_4^+-N, nitrate (NO_3^--N) and nitrite (NO_2^--N). All experiments were conducted in triplicate.

The NH_4^+-N removal efficiency was calculated by the equation: $Rv=[(T_1-T_2)/T_1]\times100.0\%$, where Rv, T_1 and T_2 represented NH_4^+-N removal efficiency, and the initial and final NH_4^+-N concentration, respectively. The heterotrophic nitrification rate and the NO_3^--N removal rate were calculated by linear fitting of the concentration changes of NO_2^--N, NO_3^--N and NO_3^--N, respectively. The heterotrophic nitrification rate was measured with 0.01% (v/v) acetylene inhibition, according to acetylene could inhibit the denitrification process and the growth of autotrophic bacteria (Ryden et al., 1987; McCarty, 1999; Lu and Jia, 2013; Zhang et al., 2014).

To detect bacterial ammonia assimilation, strain MA-ZP17-13 was cultured in HNM at 150 r/min and 10°C for 72 h in 100 mL flask. After centrifugation and freeze-drying, the intracellular N content was detected by elemental analyzer EL-III (Vario EL-III). The intracellular N content was calculated by the formula as follows: $R=R_1\times M/V$, where R (mg/L), R_1 (%), M (mg) and V (L) represented NH_4^+-N/NH_3-N concentration, the percentage of nitrogen content, dry weight, and medium volume, respectively.

2.4 *Quantification methods of NH_4^+, NO_2^- and NO_3^-*

The concentrations of NH_4^+-N, NO_2^--N and NO_3^--N were detected using the supernatant after samples centrifuged at 8 000 r/min for 5 min. The concentrations of NH_4^+-N, NO_3^--N and NO_2^--N were determined according to standard methods (APHA, 2005). The NH_4^+-N concentration was analyzed by the method of Nessler's reagent spectrophotometry. The NO_3^--N concentration was calculated by subtracting two times the background absorbance value at 275 nm from the absorbance value at 220 nm. NO_2^--N was determined at wavelengths of 540 nm after adding 1 mL chromogenic reagent including 0.1 mL phosphoric acid, 0.002 g N-(1-naphthyl)-1,2-diaminoethane dihydrochloride and 0.04 g sulfanilamide (APHA, 2005). In addition, N_2O and N_2 were detected on a gas chromatography equipped with a thermal conductivity detector and electron capture detector, respectively (Zhao et al., 2012).

2.5 *Genomic DNA preparation*

For genome sequencing, strain MA-ZP17-13 was grown aerobically to mid logarithmic phase at 10°C on marine agar 2216 medium. Genomic DNA was isolated from the cell pellets using the ChargeSwitch® gDNA Mini Bacteria Kit (Life Technologies) according to the manufacturer's instructions. Purified genomic DNA was quantified by TBS-380 fluorometer (Turner BioSystems, CA). High quality DNA ($OD_{260/280}$ is 1.8–2.0, >10 μg) was used to

do further research.

2.6 *Genome sequencing and analysis*

The genome of strain MA-ZP17-13 was sequenced using a combination of PacBio *RS* and Illumina sequencing platforms. The Illumina data was used to evaluate the complexity of the genome. These data were tried to be assembled using Velvet assembler (v1.2.09) with a k-mer length of 17 (Zerbino, 2010). The complete genome sequence was assembled using both the PacBio reads and Illumina reads. The assembly was produced firstly using a hybrid *de novo* assembly solution modified by Koren (Koren et al., 2012), in which a *de-Bruijn* based assembly algorithm and a CLR (continuous long reads) reads correction algorithm were integrated in "PacBioToCA with Celera Assembler" pipeline (Chin et al., 2013). The last circular step was checked and finished manually. The final assembly generated a circular genome sequence with no gap. The complete genome sequence was submitted to GenBank under accession No. CP034367.

Identification of predicted coding sequences (CDS), also called open reading frames (ORFs), was performed using Glimmer version 3.02. ORFs with less than 300 bp were discarded. Then remaining ORFs were queried against the non-redundant (NR) protein database in the National Center for Biotechnology Information (NCBI), SwissProt (http://uniprot.org), Kyoto Encyclopedia of Genes and Genomes (KEGG, http://www.genome.jp/kegg/), Gene Ontology (GO, http://geneontology.org) and Phylogenetic Classification of Proteins Encoded in Complete Genomes (COG, http://www.ncbi.nlm.nih.gov/COG) databases for functional annotation. In addition, plasmids were identified using the GeneMarkS (v4.30), tRNAs were identified using the tRNAscan-SE (v1.3.1) and rRNA were determined using Barrnap (v0.4.2). Circos software was then used to generate a circularized map of the chromosome, setting the calculation window at 2 000 bp with steps of 500 bp (Krzywinski et al., 2009).

Gene prediction and annotation were performed using the NCBI prokaryotic genome annotation pipeline (Tatusova et al., 2016) and six large databases (NR, Swiss-Prot, Pfam, COG, GO, and KEGG). The functional annotation of predicted ORFs was used to search the KEGG and COG databases by RPS-BLAST.

2.7 *Bacterial identification based on whole genomic sequences*

The average nucleotide identity (ANI) between strains MA-ZP17-13 and *H. venusta* DSM 4743^T was calculated with EZGenome using the algorithm of Goris et al. (2007). DNA-DNA hybridization (DDH) estimate values between two strains were analyzed using the genome-to-genome distance calculator (GGDC2.0) (Auch et al., 2010a, b; Meier-Kolthoff, et al., 2013).

2.8 *Optimization of cultivation parameters using response surface methodology*

The critical factors affecting NH_4^+-N removal efficiency, including C/N concentration ratio, pH, salinity and temperature, were screened by single-factor experiment.

Based on the preliminary results, the appropriate range of independent variables including C/N concentration ratio (A), pH (B), salinity (C) and temperature (D) were determined. The response surface methodology is an important math-statistics technique for designing, modeling and analysis of problems where a response of interest is affected by several different parameters (Qu et al., 2017). Design expert 8.0.5b software was used for the design of the experimental run (Myers et al., 2016). Box-Behnken design (BBD) was applied to generate the design matrix of four factors at three levels (Table 1). Twenty-nine BBD trials were conducted to provide direction for further optimization studies (Table 2). Analysis of variance (ANOVA) was used to check the validity of regression model and determine the quadratic effect of machine parameters on the output response function.

Statistical model analysis was evaluated to determine the ANOVA and the quadratic models were constituted as 3D contour plots using Design-Expert® 8 software (Myers et al., 2016).

3 Results and discussion

3.1 *Identification of strain MA-ZP17-13*

A nearly full-length 16S rRNA gene sequence (1 540 nt) of strain MA-ZP17-13 was determined, which showed the highest sequence similarity to *H. venusta* DSM 4743^T (99.93%), followed by *H. hydrothermalis* Slthf2^T (99.79%) and *H. alkaliphila* 18bAG^T (99.73%). A phylogenetic tree was constructed based on the 16S rRNA gene sequences of the genus *Halomonas* (Fig. 1), which showed that strain MA-ZP17-13 formed a clade with *H. venusta* DSM 4743^T. The data DNA-DNA hybridization estimate value between strain MA-ZP17-13 and *H. venusta* DSM 4743^T was 90.80%, which was above the standard cut-off value (70%) (Wayne et al., 1987). The ANI value between strain MA-ZP17-13 and *H. venusta* DSM 4743^T was 98.78%, which was above the standard ANI criteria for species identity (95%–96%) (Richter and Rosselló-Móra, 2009). Hence, strain MA-ZP17-13 was identified as *H. venusta* based on 16S rRNA gene sequence analyses and dDDH value.

On marine agar 2216, colonies of strain MA-ZP17-13 are milk white, opaque, convex, regular with entire margin and 1.0–2.0 mm in diameter after 2 d at 28°C. General features of strain MA-ZP17-13 are summarized in Table 3.

The strain is positive for catalase and oxidase, reduction of nitrate and denitrification, and is negative for arginine dihydrolase, indole production, D-glucose fermentation, urease, β-galactosidase. API ZYM test strip results indicate that it is positive for alkaline phosphatase, esterase (C4), lipase (C14), leucine aminopeptidase, naphtol-AS-BI-phosphoamidase, valine aminopeptidase, acid phosphatase, α-glucosidase; it is weakly positive for esterase lipase (C8), cystine aminopeptidase; it is negative for N-acetyl-β-glucosaminidase, trypsin, α-chymotrypsin, α-galactosidase, β-galactosidase, β-glucuronidase, β-glucosidase, α-fucosidase and α-mannosidase. The API 20NE test strip shows that strain MA-ZP17-13 can utilize D-glucose, D-mannitol, D-maltose, N-acetyl-glucosamine, potassium gluconate, capric acid, adipic acid, malic acid, trisodium citrate and phenylacetic acid, cannot utilize L-arabinose and D-mannose.

Table 1. Real and coded variables used to optimize ammonia nitrogen removal in BBD

Factor	Name	Level	Low level	High level
A	C/N concentration ratio	4.0	2.0	6.0
B	pH	7.5	6.0	9.0
C	NaCl/%	2.5	0.0	5.0
D	temperature/°C	10.0	5.0	15.0

Table 2. Experimental design and result of full model BBD for response

Run	Independent variables				Response
	A C/N concentration ratio	B pH	C NaCl/%	D Temperature /°C	Ammonia removal Y1/%
1	2	6	2.5	10	40.3
2	6	6	2.5	10	62.5
3	2	9	2.5	10	52.4
4	6	9	2.5	10	100.0
5	4	7.5	0	5	68.0
6	4	7.5	5	5	36.2
7	4	7.5	0	15	70.3
8	4	7.5	5	15	68.0
9	2	7.5	2.5	5	36.0
10	6	7.5	2.5	5	50.1
11	2	7.5	2.5	15	37.5
12	6	7.5	2.5	15	83.9
13	4	6	0	10	59.8
14	4	9	0	10	84.4
15	4	6	5	10	54.9
16	4	9	5	10	77.7
17	2	7.5	0	10	51.0
18	6	7.5	0	10	87.7
19	2	7.5	5	10	43.1
20	6	7.5	5	10	82.4
21	4	6	2.5	5	18.5
22	4	9	2.5	5	59.3
23	4	6	2.5	15	40.0
24	4	9	2.5	15	74.2
25	4	7.5	2.5	10	67.0
26	4	7.5	2.5	10	67.0
27	4	7.5	2.5	10	67.0
28	4	7.5	2.5	10	67.0
29	4	7.5	2.5	10	67.0

3.2 *Determination of the NH_4^+-N/NH_3-N removal rate and transformation capacity of strain MA-ZP17-13*

Low temperature can reduce NH_4^+-N/NH_3-N removal rate by slowing down microbial growth (Zhang et al., 2011; Rodriguez-Caballero et al., 2012; Huang et al., 2013). To determine the NH_4^+-N/NH_3-N removal efficiency of strain MA-ZP17-13 at 10°C, 100 mg/L initial concentration of NH_4^+-N/NH_3-N was used as the sole nitrogen source in HNM medium. The NH_4^+-N/NH_3-N concentration showed a significant decrease from 100.0 mg/L to 11.2 mg/L, with about 90% of NH_4^+-N/NH_3-N removal after 72 h of incubation at 10°C, and the average NH_4^+-N/NH_3-N removal rate was approximately 1.23 mg/(L·h) (Fig. 2). With the increase of culture time, NH_4^+-N/NH_3-N could not be removed completely, but it could be decreased to 3 mg/L within 120 h. *Microbacterium* sp. SFA13 was reported to have the ability of NH_4^+-N/NH_3-N removal, with an average removal rate of 0.11 mg/(L·h) at 5°C (Zhang et al., 2013). Strain MA-ZP17-13 showed a high potential for NH_4^+-N/NH_3-N removal at low temperature. Therefore, this strain has important application potential in sewage treatment of NH_4^+-N/NH_3-N removal under low temperature.

The NH_4^+-N/NH_3-N removal in the medium is supposed to be carried out via assimilation and/or nitrification. To detect the amount of NH_4^+-N/NH_3-N assimilation, strain MA-ZP17-13 was cultured in HNM medium at the initial concentration of 100 mg/L NH_4^+-N, at 150 r/min and 10°C for 72 h. After centrifuging and freeze-drying, the average dry weight of three parallel samples was 48.4 mg. The average percentage of nitrogen concentration is 10.4%. After calculation by the equation $R=R_1\times M/V$, the NH_4^+-N/NH_3-N assimilated by strain MA-ZP17-13 was 50.3 mg/L on average.

To determine nitrification efficiency of this bacterium at low temperature, ammonia was used as the only N source in HNM medium under aerobic conditions at 10°C, with an initial concentration of 100 mg/L NH_4^+-N/NH_3-N. The slope of the linear line of best fit was equal to the heterotrophic nitrification rate (Fig. 3). The heterotrophic nitrification rate was 0.016 6 mg/(L·h).

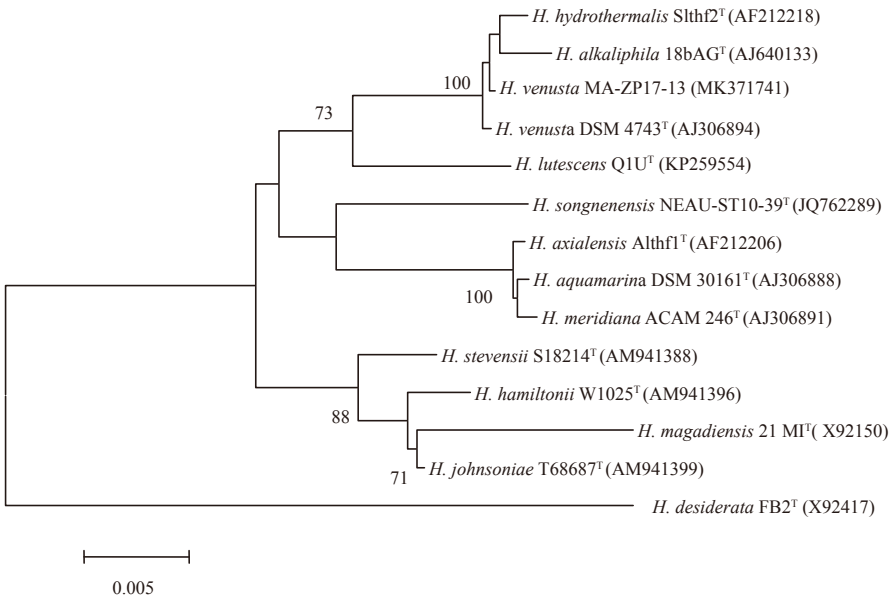

Fig. 1. Neighbour-joining tree showing the phylogenetic positions of strain MA-ZP17-13 and other members of the genus *Halomonas*, based on 16S rRNA gene sequences. The bootstrap values on the branching nodes were calculated on 1 000 replications. The scale bar indicated 0.005 substitutions per nucleotide position.

Table 3. General features of strain MA-ZP17-13 and MIGS mandatory information

Items	Description
General features	
Classification	domains: Bacteria, phylum: Proteobacteria, class: Gammaproteobacteria, order: Oceanospirillales, family: Halomonadaceae, genus: *Halomonas*, species: *Halomonas venusta*
Gram stain	negative
Cell shape	rod
Motility	motile
Pigmentation	no-pigment
Temperature range/°C	4–55
Optimum temperature/°C	28–37
Energy source	chemoorganotrophic
Terminal electron receptor	oxygen
Oxygen	aerobic
NaCl content/%	0–15
pH	5.0–10.0
MIGS data	
Submitted to INSDC	GenBank (ID: CP034367)
Investigation type	bacteria
Project name	*Halomonas venusta* strain: MA-ZP17-13 genome sequencing
Geographic location (country)	China
Collection date	2018
Environment (biome)	seawater farms
Environment (feature)	water
Environment (material)	seawater
Environmental package	mariculture samples from Zhangzhou, China
Biotic relationship	free-living
Pathogenicity	none
Sequencing method	PacBio RS, Illumina Hiseq2000
Assembly	GS *De Novo* Assembler package
Finishing strategy	complete

Note: INSDC represents International Nucleotide Sequence Database Collaboration.

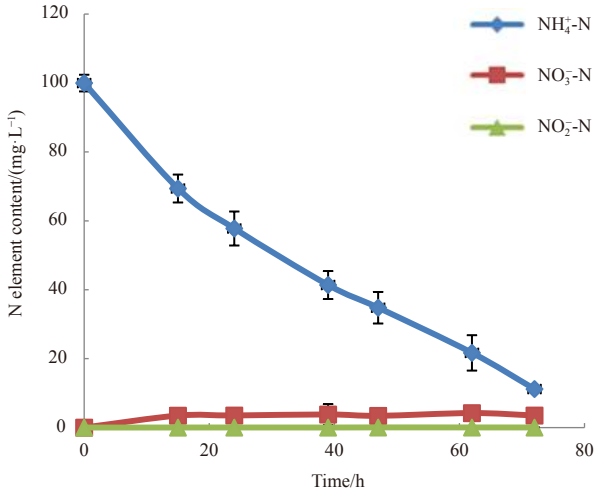

Fig. 2. Ammonium-nitrogen removal rate of strain *Halomonas venusta* MA-ZP17-13.

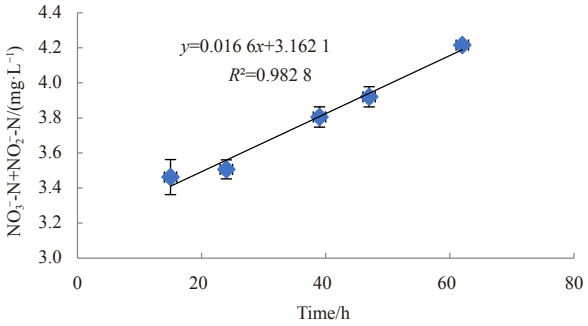

Fig. 3. The accumulation of NO_3^--N and NO_2^--N of strain *H. venusta* MA-ZP17-13 under heterotrophic nitrification condition at low temperature.

The average NH_4^+-N/NH_3-N assimilated by the isolate was 50.3 mg; so the NH_4^+-N/NH_3-N removed by heterotrophic nitrification, in theory, is approximately 49.5 mg, which would result in a calculated heterotrophic nitrification rate of 0.69 mg/(L·h). There was a 40-fold difference between the two calculation methods. The actual nitrification capacity should be higher than the measured value because the strain also had denitrification capacity (Fig. 4). In addition, acetylene inhibits the oxidation of NH_4^+-N/NH_3-N to NO_2^--N (Hynes and Knowles, 1978). The calculated heterotrophic nitrification rate of 0.69 mg/(L·h) is expected to be close to the actual value.

To determine its NO_3^--N removal capacity at 10°C, an initial concentration of 150 mg/L NO_3^--N was used as sole N source in DM medium. Incubation under aerobic conditions resulted in a significant decrease in the NO_3^--N concentration (Fig. 4a). The rate of decrease of NO_3^--N was determined by linear fitting, where the slope of linear fitting is the removal rate. The NO_3^--N

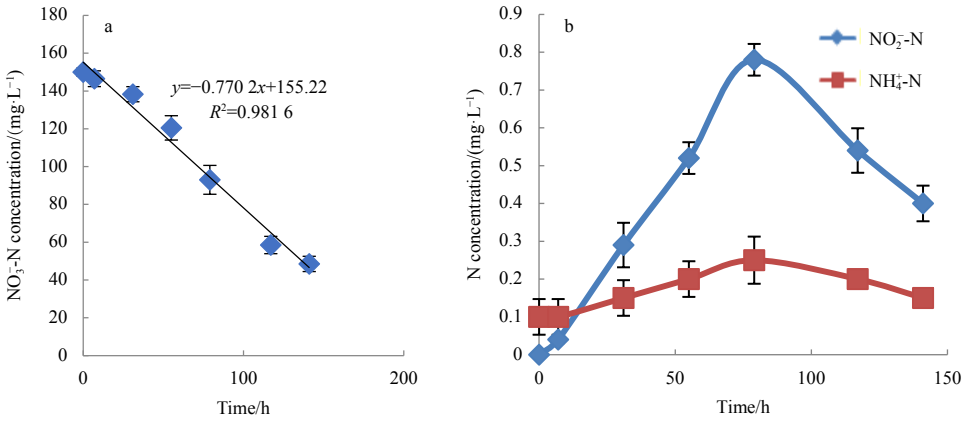

Fig. 4. The dynamic changes of NO_3^--N, NO_2^--N and NH_4^+-N during denitrification process. a. Removal rate of NO_3^--N by strain MA-ZP17-13; b. the dynamic changes ofNO_2^--N and NH_4^+-N concentrations during denitrification.

removal rate of strain MA-ZP17-13 was 0.77 mg/(L·h). To clarify the denitrifying ability of strain MA-ZP17-13, changes of the NO_2^--N and NH_4^+-N/NH_3-N concentrations were also detected; with the decrease in NO_3^--N concentration, the NO_2^--N concentration increased in the first 79 h, and then rapidly decreased to low concentration of about 0.3 mg/L (Fig. 4b). Unlike NO_2^--N, the NH_4^+-N/NH_3-N concentrations was low and showed no significant change throughout the process. In addition, only N_2O was observed as the end product of denitrification, no N_2 was detected under aerobic conditions.

In conclusion, strain MA-ZP17-13 is capable of SND under low temperature. Compared with traditional denitrifying strains, SND has advantages such as high NH_4^+-N/NH_3-N removal efficiency, fast microbial growth, and low process costs (Zhu et al., 2008; Wang et al., 2019). Therefore, the research on SND is of great significance to the sewage treatment industry.

3.3 *Optimization of ammonia removal conditions*

3.3.1 *Development of regression model equations*

Based on the single-factor experiments, a complete experimental design matrix was developed by BBD for further optimizations of the four parameters. The values of the response gained from the experiment were shown in Table 2. The NH_4^+-N/NH_3-N removal percentage *R*1 ranged from 18.5% to 100.0%. For these responses, the empirical quadratic model was applied as recommendation for BBD to develop the correlation between the responses and independent variables as follows:

$$R1 = 67.0 + 17.19A + 14.33B - 4.91C + 8.82D + 6.35AB + 0.65AC + 8.07AD - 0.45BC - 1.65BD + 7.38CD - 2.56A^2 - 2.92B^2 + 4.51C^2 - 13.18D^2. \quad (1)$$

The accuracy of the established regression models was then assessed by the correlation coefficient R^2, with values closer to 1, indicating a more precise response value estimated by the models. The R^2 value for Eq. (1) was 0.96 and the predicted values versus the corresponding experimental values for Y1 were shown in Fig. 5. As expected, the actual values were consistent with the predicted values, implying that the models successfully predicted the relationships between culture parameters and NH_4^+-N/NH_3-N removal.

In addition to the correlation coefficients, *F*-values and *P*-values were employed to determine the significance of the models

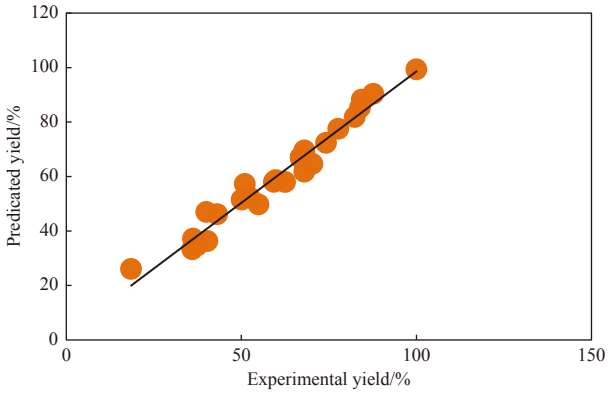

Fig. 5. Predicted vs. experimental values of ammonia nitrogen removal.

and each model term, with a larger *F*-value indicating increased significance of the corresponding coefficient (Zhou et al., 2013). The ANOVA of the predicted quadratic model for NH_4^+-N/NH_3-N removal (Table 4) showed that the model was statistically significant (*F*-value=27.57), indicating that most of the variations in the response could be explained with the regression equation. $P<0.05$ implied that the model terms were significant (Savasari et al., 2015). In this case, A (C/N concentration ratio), B (pH), C (NaCl), D (temperature), AB, AD, CD, the quadratic terms of salinity C^2 and the quadratic terms of temperature D^2 were significant.

3.3.2 *Ammonia nitrogen removal process*

The NH_4^+-N/NH_3-N removal capacities of strain MA-ZP17-13 for different combinations of the independent preparation parameters were visualized through 3D response surface plots (Fig. 6). The interactive effect between A (C/N concentration ratio) and B (pH) was observed (Fig. 6a), and confirmed by the corresponding *F*-value (6.65) and *P* (0.021 9; Table 4). The upward trend in NH_4^+-N/NH_3-N removal was attributed to the increasing degree of A (C/N concentration ratio) and B (pH), with higher values of A and B resulting in higher NH_4^+-N/NH_3-N removal rate. The interactive effect of A (C/N concentration ratio) and C (NaCl) on the NH_4^+-N/NH_3-N removal rate was shown in Fig. 6b. The curved contour lines demonstrated that the increase in NH_4^+-N/NH_3-N removal was attributed to the decrease in C (NaCl) and the increase in A (C/N concentration ratio). Similarly, a relatively strong interaction was identified between A (C/N concentration

Table 4. ANOVA of the response surface quadratic model for ammonia nitrogen removal

Source	Sum of squares	Degree of freedom	Mean square	*F*-value	*P*
Model	9 366.15	14	669.01	27.57	<0.000 1
A (C/N concentration ratio)	3 546.64	1	3 546.64	146.17	<0.000 1
B (pH)	2 465.33	1	2 465.33	101.61	<0.000 1
C (NaCl)	289.10	1	289.10	11.92	0.003 9
D (temperature)	932.80	1	932.80	38.45	<0.000 1
AB	161.29	1	161.29	6.65	0.021 9
AC	1.69	1	1.69	0.07	0.795 7
AD	260.82	1	260.82	10.75	0.005 5
BC	0.81	1	0.81	0.03	0.857 6
BD	10.89	1	10.89	0.45	0.513 8
CD	217.56	1	217.56	8.97	0.009 7
A^2	42.59	1	42.59	1.76	0.206 4
B^2	55.50	1	55.50	2.29	0.152 7
C^2	132.08	1	132.08	5.44	0.035 1
D^2	1 125.93	1	1 125.93	46.40	<0.000 1
Residual	339.68	14	24.26	–	–

Note: –, no data.

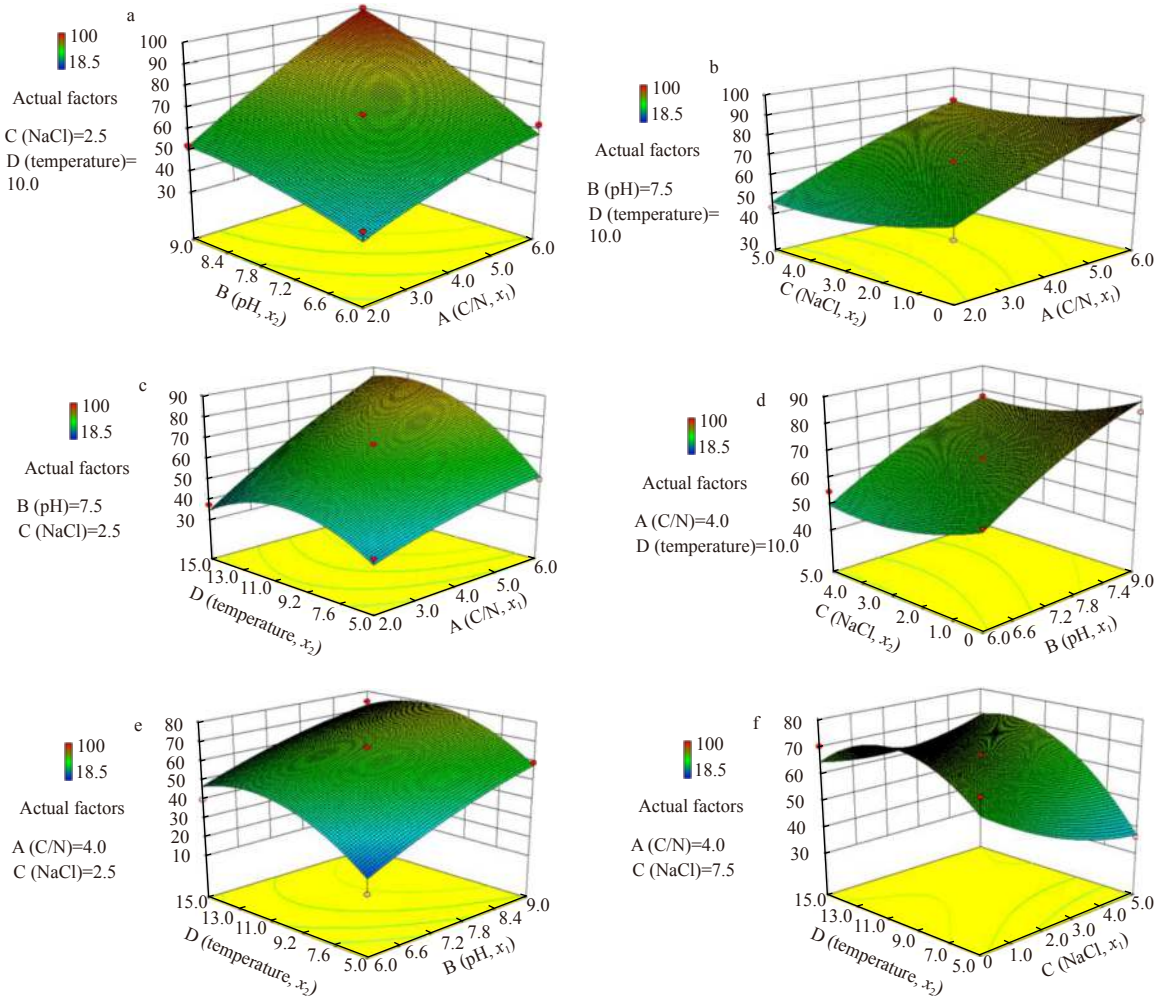

Fig. 6. The interactions and response surfaces of the culture parameters for the ammonia nitrogen removal.

ratio) and D (temperature) on NH_4^+-N/NH_3-N removal rate (Fig. 6c). During the initial stage, as these two factors increased, there is a simultaneous increase in the NH_4^+-N/NH_3-N removal rate. Thereafter, a continued increase in D (temperature) lead to a reduction in the NH_4^+-N/NH_3-N removal capacity, which indicates that strain MA-ZP17-13 is psychrophilic. There is a significant interactive effect between B (pH) and C (NaCl) on NH_4^+-N/NH_3-N removal (Fig. 6d). The upward trend in NH_4^+-N/NH_3-N removal

was attributed to the slow decrease in C (NaCl) and the increase in B (pH). Salinity alone had little effect on NH_4^+/NH_3 removal (confirmed by the corresponding *F*-value (11.92) and *P* (0.003 9) in (Table 4). There was an interactive effect between pH (B) and temperature (D) on NH_4^+-N/NH_3-N removal (Fig. 6e). During the initial stage, as these two factors (NaCl and temperature) increased, NH_4^+-N/NH_3-N removal increased. Thereafter, a continued increase in D (temperature) led to a slow downward trend in the NH_4^+-N/NH_3-N removal capacity. Finally, there was an interactive effect between C (NaCl) and D (temperature) on NH_4^+-N/NH_3-N removal (Fig. 6f). With the increase of these two factors, NH_4^+-N/NH_3-N removal slowly increased, because the NH_4^+-N/NH_3-N removal capacity was negatively correlated with concentration of NaCl (C). The higher the salinity, the lower the NH_4^+-N/NH_3-N removal capacity. When C (NaCl) was 0, the increase in D (temperature) in the first stage resulted in increased NH_4^+-N/NH_3-N removal capacity until the optimal level was reached; NH_4^+-N/NH_3-N removal capacity then decreased with the increase in D (temperature) above the optimal value.

3.3.3 *Process optimization*

The NH_4^+-N/NH_3-N removal capacity was significantly influenced by four culture parameters of C/N ratio (A), pH (B), NaCl (C) and temperature (D). Although the influences of these four parameters were different, it was possible to balance the responses by searching for the optimum point. The optimal *R*1 was obtained using the following conditions: C/N ratio at 5.95, pH 8.93, NaCl at 2.33% and temperature at 11.2°C, which could result in 100% NH_4^+-N/NH_3-N removal according to the regression models. Verification of the predictive results were carried out by three independent experiments under the predicted optimal conditions. The average experimental NH_4^+-N/NH_3-N removal capacity (98.7%±0.9%) was similar to the values predicted from the models, with a small errors of 1.33%. Through process optimization, the NH_4^+-N/NH_3-N removal rate was greatly increased from 88.0% to 98.7%, with the average NH_4^+-N/NH_3-N removal rate of 1.37 mg/(L·h).

The NH_4^+-N/NH_3-N removal ability of strain MA-ZP17-13 at low temperature was comparable to other previously reported bacteria, which were isolated from sediment, groundwater and soil, and the ammonia nitrogen removal rate were in the range of 0.092–3.03 mg/(L·h) (Table 5) (Huang et al., 2013; Yao et al., 2013; Qu et al., 2015). Compared with the above strains, strain MA-ZP17-13 had higher salinity tolerance, because it came from aquaculture seawater.

3.4 *Genes and pathways involved nitrogen metabolisms based on the complete genomic sequencing*

The complete genome sequence of strain MA-ZP17-13 was determined in this study. It consisted of one chromosome with a total length of 4 446 698 bp with a G+C content of 52.79% (according to amount of substance) (Fig. 7). Gene prediction identified 4 330 genes, of which 4 251 were CDSs, and 79 were RNAs

Table 5. Comparison with other studies of ammonia nitrogen removal at low temperature

Strain name	Source	Salinity	Temperature/°C	RTAM/(mg·L^{-1}·h^{-1})	Reference
Acinetobacter sp. HA2	sediment	0	10.0	3.03	Yao et al. (2013)
Acinetobacter sp. Y16	water	0.12	2.0	0.092	Huang et al. (2013)
Pseudomonas migulae AN-1	water	0	10.0	1.56	Qu et al. (2015)
Pseudomonas putida Y-9	soil	0	15.0	2.85	Xu et al. (2017)
H. venusta MA-ZP17-13	seawater	23.3	11.2	1.37	present study

Note: RTAM represents removal rate of total ammonia nitrogen.

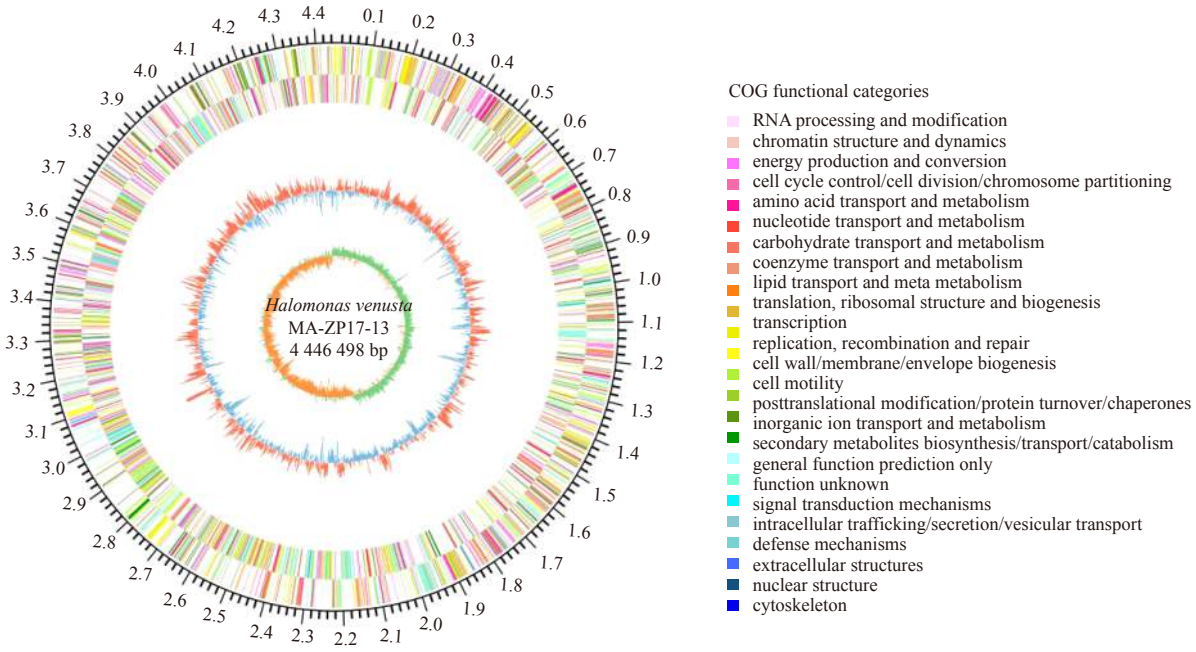

Fig. 7. Circular representation of *Halomonas venusta* MA-ZP17-13 genome. From the outside to the center: label of genome size (Mbp), CDSs on forward strand (colored by COG categories), CDSs on reverse strand (colored by COG categories), G+C content and GC skew. CDSs are depicted in different colors according to COG categories.

Table 6. Genome statistics of *Halomonas venusta* MA-ZP17-13

Attribute	Genome (total) value	Proportion of total/%
Genome size/bp	4 446 698	100.00
G+C content/bp	2 347 412	52.79
Coding region/bp	3 979 236	89.49
TandemRepeat/bp	60 444	1.52
Total genes	4 330	100.00
RNA genes	79	1.82
rRNA operons	18	0.42
tRNA genes	61	1.41
Protein-coding genes	4 251	98.18
Genes assigned to COGs	3 676	86.47

(Table 6). The average length of the CDSs was 936 bp, giving a coding density of 96.0%. To further understand the adaptive capacity of strain MA-ZP17-13 to the aquaculture environment, metabolic features related to functional categories were analyzed. Twenty-five genes were found relating to N metabolism, which included nitrification and denitrification (Supplementary Table S1).

Genes encoding ammonia monooxygenase, nitric oxide dioxygenase, nitric oxide synthase, nitrite reductases, nitrate reductases and dissimilatory nitrite reductases were present in the genome of this strain, indicating that it was capable for both nitrification and denitrification. Consistent with its NH_4^+-N/NH_3-N removal activity, the genome of *H. venusta* MA-ZP17-13 contained an ammonia monooxygenase gene (MA-ZP17-13_3 189), which is 1 041 bp long and encodes 346 amino acids. Interestingly, the genome contained no hydroxylamine oxidase gene, which raises questions about the nitrification process of strain MA-ZP17-13. Nitric oxide dioxygenases (NODs) were present in the genome. NODs catalyze the reaction of O_2 and NO to yield NO_3^- (Gardner et al., 1998; Lundberg et al., 2004; Schopfer et al., 2009). Therefore, this study inferred that there might be a new nitrification pathway in strain MA-ZP17-13, and the specific pathway was speculated as follows: $NH_4^+ \rightarrow NH_2OH \rightarrow NO \rightarrow NO_3^-$.

Consistent with the abilities of strain MA-ZP17-13, *H. alkaliphila* X3^T was reported to be capable for heterotrophic nitrification-aerobic denitrification (Zhang et al., 2016) and the genome was obtained from NCBI database. These strains shared 99.68% similarity in 16S rRNA gene sequence, but the ANI between the two strains was 93.01%, indicating that the two strains belonged to two different species in genus *Halomonas*. This study found that *H. alkaliphila* X3^T possessed similar nitrification-related genes and was also lacking hydroxylamine oxidase. The ammonia monooxygenase gene in strain MA-ZP17-13 is also 1 041 bp long and encodes 346 amino acids and is homologous to the corresponding gene in strain X3^T with at least 99% amino acid identity. The high sequence similarity of the ammonia monooxygenase gene between strains MA-ZP17-13 and *H. alkaliphila* X3^T indicates similar function and regulation of NH_4^+-N/NH_3-N oxidation.

In addition, this study found that the same gene cluster of nitrate reductase was present in strains MA-ZP17-13 and *H. alkaliphila* X3^T. The gene cluster contains the nitrate reductase gamma subunit (*narI*), nitrate reductase molybdenum cofactor assembly chaperone (*narJ*), nitrate reductase subunit beta (*narH*), nitrate reductase subunit alpha (*narG*), nitrate/nitrite sensor protein (*narX*), DNA-binding response regulator (*narL*), and MFS transporter (*narK*) genes (Fig. 8). Genes of nitrite reductases, nitrate reductases, nitric oxide dioxygenase, nitric oxide synthase, dissimilatory nitrite reductases were present in both strain MA-ZP17-13 and X3^T. Validation of the function of these encoding genes requires further study to confirm their abilities and determine the mechanism of nitrification and denitrification, which is currently unknown. Increased understanding of the mechanisms of NH_4^+-N/NH_3-N removal in this strain could aid in developing strategies for bioremediation of NH_4^+-N/NH_3-N pollution.

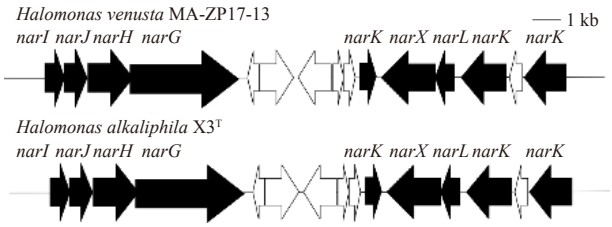

Fig. 8. Gene cluster of nitrate reducase of *Halomonas venusta* MA-ZP17-13 and *Halomonas alkaliphila* X3^T. *narI*: nitrate reductase, gamma subunit; *narJ*: nitrate reductase molybdenum cofactor assembly chaperone; *narH*: nitrate reductase subunit beta; *narG*: nitrate reductase subunit alpha; *narX*: nitrate/nitrite sensor protein; *narL*: DNA-binding response regulator; *narK*: MFS transporter.

4 Conclusions

The isolated *Halomonas venusta* MA-ZP17-13 is capable for NH_4^+-N/NH_3-N removal via assimilation at 0.7 mg/(L·h), and also performs simultaneous heterotrophic nitrification and denitrification under aerobic conditions. Quantification results showed that about half of NH_4^+-N/NH_3-N was removed by assimilation, and half was removed by denitrification firstly via nitrification. The optimal ammonia removal conditions were determined as C/N concentration ratio 5.95, pH 8.93, 2.33% NaCl and 11.2°C, which lead to 98.7% NH_4^+-N/NH_3-N removed in 72 h at the initial concentration of 100 mg/L and the removal rate averaged at 1.37 mg/(L·h) (according to N). The ammonia removal potential is also supported by the presence of genes encoding ammonia monooxygenase, respiratory nitrate reductase, nitrite reductase, nitric oxide synthase and nitric oxide dioxygenase in the genome though the gene hydroxylamine oxidase was found in the complete genome sequence. This supposed a potential novel nitrification pathway of $NH_4^+ \rightarrow NH_2OH \rightarrow NO \rightarrow NO_3^-$ and needs further investigation. Together, these results indicate that this bacterium has potential for NH_4^+-N/NH_3-N removal in salty water at low temperature.

References

APHA. 2005. Standard Methods for the Examination of Water and Wastewater. 21th ed. Washington, DC, USA: American Public Health Association (APHA)

Armstrong D A, Chippendale D, Knight A W, et al. 1978. Interaction of ionized and un-ionized ammonia on short-term survival and growth of prawn larvae, *Macrobrachium rosenbergh*. The Biological Bulletin, 154(1): 15–31, doi: 10.2307/1540771

Atanassov C L, Muller C D, Sarhan S, et al. 1994. Effect of ammonia on endocytosis, cytokine production and lysosomal enzyme activity of a microglial cell line. Research in Immunology, 145(4): 277–288, doi: 10.1016/S0923-2494(94)80016-2

Auch A F, Klenk H P, Göker M. 2010a. Standard operating procedure for calculating genome-to-genome distances based on high-scoring segment pairs. Standards in Genomic Sciences, 2(1): 142–148, doi: 10.4056/sigs.541628

Auch A F, Von Jan M, Klenk H P, et al. 2010b. Digital DNA-DNA hybridization for microbial species delineation by means of gen-

ome-to-genome sequence comparison. Standards in Genomic Sciences, 2(1): 117–134, doi: 10.4056/sigs.531120

Carrera J, Vicent T, Lafuente F J. 2003. Influence of temperature on denitrification of an industrial high-strength nitrogen wastewater in a two-sludge system. Water SA, 29(1): 11–16

Chen Qian, Ni Jinren. 2012. Ammonium removal by *Agrobacterium* sp. LAD9 capable of heterotrophic nitrification–aerobic denitrification. Journal of Bioscience and Bioengineering, 113(5): 619–623, doi: 10.1016/j.jbiosc.2011.12.012

Chin C S, Alexander D H, Marks P, et al. 2013. Nonhybrid, finished microbial genome assemblies from long-read SMRT sequencing data. Nature Methods, 10(6): 563–569, doi: 10.1038/nmeth.2474

Chiu Y C, Lee L L, Chang Chengnan, et al. 2007. Control of carbon and ammonium ratio for simultaneous nitrification and denitrification in a sequencing batch bioreactor. International Biodeterioration & Biodegradation, 59(1): 1–7

Gardner P R, Gardner A M, Martin L A, et al. 1998. Nitric oxide dioxygenase: an enzymic function for flavohemoglobin. Proceedings of the National Academy of Sciences of the United States of America, 95(18): 10378–10383, doi: 10.1073/pnas.95.18.10378

Goris J, Konstantinidis K T, Klappenbach J A, et al. 2007. DNA–DNA hybridization values and their relationship to whole-genome sequence similarities. International Journal of Systematic and Evolutionary Microbiology, 57(1): 81–91, doi: 10.1099/ijs.0.64483-0

He Tengxia, Li Zhenlun, Sun Quan, et al. 2016. Heterotrophic nitrification and aerobic denitrification by *Pseudomonas tolaasii* Y-11 without nitrite accumulation during nitrogen conversion. Bioresource Technology, 200: 493–499, doi: 10.1016/j.biortech.2015.10.064

He Tengxia, Xie Deti, Li Zhenlun, et al. 2017. Ammonium stimulates nitrate reduction during simultaneous nitrification and denitrification process by *Arthrobacter arilaitensis* Y-10. Bioresource Technology, 239: 66–73, doi: 10.1016/j.biortech.2017.04.125

Hooper A B, Vannelli T, Bergmann D J, et al. 1997. Enzymology of the oxidation of ammonia to nitrite by bacteria. Antonie van Leeuwenhoek, 71(1): 59–67

Huang Xiaofei, Li Weiguang, Zhang Duoying, et al. 2013. Ammonium removal by a novel oligotrophic *Acinetobacter* sp. Y16 capable of heterotrophic nitrification-aerobic denitrification at low temperature. Bioresource Technology, 146: 44–50, doi: 10.1016/j.biortech.2013.07.046

Hynes R K, Knowles R. 1978. Inhibition by acetylene of ammonia oxidation in *Nitrosomonas europaea*. FEMS Microbiology Letters, 4(6): 319–321, doi: 10.1111/j.1574-6968.1978.tb02889.x

Kan Fu, Xia Qinbin, Li Zhong, et al. 2011. Research of ammonia adsorption with Maifan stone. Industrial Safety and Environmental Protection, 37(4): 3–5

Kim J K, Park K J, Cho K S, et al. 2005. Aerobic nitrification–denitrification by heterotrophic *Bacillus* strains. Bioresource Technology, 96(17): 1897–1906, doi: 10.1016/j.biortech.2005.01.040

Koren S, Schatz M C, Walenz B P, et al. 2012. Hybrid error correction and *de novo* assembly of single-molecule sequencing reads. Nature Biotechnology, 30(7): 693–700, doi: 10.1038/nbt.2280

Krzywinski M, Schein J, Birol I, et al. 2009. Circos: an information aesthetic for comparative genomics. Genome Research, 19(9): 1639–1645, doi: 10.1101/gr.092759.109

Li Guizhen, Lai Qiliang, Yan Peisheng, et al. 2019. *Roseovarius amoyensis* sp. nov. and *Muricauda amoyensis* sp. nov., isolated from the Xiamen coast. International Journal of Systematic and Evolutionary Microbiology, 69(10): 3100–3108, doi: 10.1099/ijsem.0.003595

Lin Y C, Chen J C. 2003. Acute toxicity of nitrite on *Litopenaeus vannamei* (Boone) juveniles at different salinity levels. Aquaculture, 224(1–4): 193–201, doi: 10.1016/S0044-8486(03)00220-5

Lu Lu, Jia Zhongjun. 2013. Urease gene-containing *Archaea* dominate autotrophic ammonia oxidation in two acid soils. Environmental Microbiology, 15(6): 1795–1809, doi: 10.1111/1462-2920.12071

Lundberg J O, Weitzberg E, Cole J A, et al. 2004. Nitrate, bacteria and human health. Nature Reviews Microbiology, 2(7): 593–602, doi: 10.1038/nrmicro929

McCarty G W. 1999. Modes of action of nitrification inhibitors. Biology and Fertility of Soils, 29(1): 1–9, doi: 10.1007/s003740050518

Meier-Kolthoff J P, Auch A F, Klenk H P, et al. 2013. Genome sequence-based species delimitation with confidence intervals and improved distance functions. BMC Bioinformatics, 14: 60, doi: 10.1186/1471-2105-14-60

Myers R H, Montgomery D C, Anderson-Cook C M. 2016. Response Surface Methodology: Process and Product Optimization Using Designed Experiments. New York: John Wiley & Sons

Qu Dan, Wang Cong, Wang Yanfang, et al. 2015. Heterotrophic nitrification and aerobic denitrification by a novel groundwater origin cold-adapted bacterium at low temperatures. RSC Advances, 5(7): 5149–5157, doi: 10.1039/C4RA13141J

Qu Jianhua, Meng Xianlin, You Hong, et al. 2017. Utilization of rice husks functionalized with xanthates as cost-effective biosorbents for optimal Cd(II) removal from aqueous solution via response surface methodology. Bioresource Technology, 241: 1036–1042, doi: 10.1016/j.biortech.2017.06.055

Ren Yongxiang, Yang Lei, Liang Xian. 2014. The characteristics of a novel heterotrophic nitrifying and aerobic denitrifying bacterium, *Acinetobacter junii* YB. Bioresource Technology, 171: 1–9, doi: 10.1016/j.biortech.2014.08.058

Richter M, Rosselló-Móra R. 2009. Shifting the genomic gold standard for the prokaryotic species definition. Proceedings of the National Academy of Sciences of the United States of America, 106(45): 19126–19131, doi: 10.1073/pnas.0906412106

Rodriguez-Caballero A, Hallin S, Påhlson C, et al. 2012. Ammonia oxidizing bacterial community composition and process performance in wastewater treatment plants under low temperature conditions. Water Science and Technology, 65(2): 197–204, doi: 10.2166/wst.2012.643

Ryden J C, Skinner J H, Nixon D J. 1987. Soil core incubation system for the field measurement of denitrification using acetylene-inhibition. Soil Biology and Biochemistry, 19(6): 753–757, doi: 10.1016/0038-0717(87)90059-9

Savasari M, Emadi M, Ali Bahmanyar M, et al. 2015. Optimization of Cd (II) removal from aqueous solution by ascorbic acid-stabilized zero valent iron nanoparticles using response surface methodology. Journal of Industrial and Engineering Chemistry, 21: 1403–1409, doi: 10.1016/j.jiec.2014.06.014

Schopfer M P, Mondal B, Lee D H, et al. 2009. Heme/O_2/·NO Nitric oxide dioxygenase (NOD) reactivity: phenolic nitration via a putative heme-peroxynitrite intermediate. Journal of the American Chemical Society, 131(32): 11304–11305, doi: 10.1021/ja904832j

Schuler D J, Boardman G D, Kuhn D D, et al. 2010. Acute toxicity of ammonia and nitrite to pacific white shrimp, *Litopenaeus vannamei*, at low salinities. Journal of the World Aquaculture Society, 41(3): 438–446, doi: 10.1111/j.1749-7345.2010.00385.x

Shan H, Obbard J. 2001. Ammonia removal from prawn aquaculture water using immobilized nitrifying bacteria. Applied Microbiology and Biotechnology, 57(5–6): 791–798, doi: 10.1007/s00253-001-0835-1

Smart G R. 1978. Investigations of the toxic mechanisms of ammonia to fish–gas exchange in rainbow trout (*Salmo gairdneri*) exposed to acutely lethal concentrations. Journal of Fish Biology, 12(1): 93–104, doi: 10.1111/j.1095-8649.1978.tb04155.x

Tatusova T, Dicuccio M, Badretdin A, et al. 2016. NCBI prokaryotic genome annotation pipeline. Nucleic Acids Research, 44(14): 6614–6624, doi: 10.1093/nar/gkw569

Thurston R V, Russo R C, Vinogradov G A. 1981. Ammonia toxicity to fishes. Effect of pH on the toxicity of the unionized ammonia species. Environmental Science & Technology, 15(7): 837–840

Wang Te, Jiang Zhengzhong, Dong Wenbo, et al. 2019. Growth and nitrogen removal characteristics of *Halomonas* sp. B01 under high salinity. Annals of Microbiology, 69(13): 1425–1433, doi: 10.1007/s13213-019-01526-y

Wayne L G, Brenner D J, Colwell R R, et al. 1987. Report of the ad hoc

committee on reconciliation of approaches to bacterial systematics. International Journal of Systematic and Evolutionary Microbiology, 37(4): 463–464, doi: 10.1099/00207713-37-4-463

Wei Yunxia, Li Yanfeng, Ye Zhengfang. 2010. Enhancement of removal efficiency of ammonia nitrogen in sequencing batch reactor using natural zeolite. Environmental Earth Sciences, 60(7): 1407–1413, doi: 10.1007/s12665-009-0276-1

Xu Yi, He Tengxia, Li Zhenlun, et al. 2017. Nitrogen removal characteristics of *Pseudomonas putida* Y-9 capable of heterotrophic nitrification and aerobic denitrification at low temperature. BioMed Research International, 2017: 1429018

Yao Shuo, Ni Jinren, Ma Tao, et al. 2013. Heterotrophic nitrification and aerobic denitrification at low temperature by a newly isolated bacterium, *Acinetobacter* sp. HA2. Bioresource Technology, 139: 80–86, doi: 10.1016/j.biortech.2013.03.189

Yu Lei, Wang Yangqing, Liu Hongjie, et al. 2016. A novel heterotrophic nitrifying and aerobic denitrifying bacterium, *Zobellella taiwanensis* DN-7, can remove high-strength ammonium. Applied Microbiology and Biotechnology, 100(9): 4219–4229, doi: 10.1007/s00253-016-7290-5

Zerbino D R. 2010. Using the Velvet *de novo* assembler for short-read sequencing technologies. Current Protocols in Bioinformatics, 31(1): 5–11

Zhang Yan, Cheng Yu, Fei Yutao, et al. 2016. Response to different nitrogen forms of heterotrophic nitrifying-aerobic denitrifying bacteria X_3. Advances in Marine Sciences, 3(4): 118–126, doi: 10.12677/AMS.2016.34016

Zhang Duoying, Li Weiguang, Huang Xiaofei, et al. 2013. Removal of ammonium in surface water at low temperature by a newly isolated *Microbacterium* sp. strain SFA13. Bioresource Technology, 137: 147–152, doi: 10.1016/j.biortech.2013.03.094

Zhang Jinbo, Sun Weijun, Zhong Wenhui, et al. 2014. The substrate is an important factor in controlling the significance of heterotrophic nitrification in acidic forest soils. Soil Biology and Biochemistry, 76: 143–148, doi: 10.1016/j.soilbio.2014.05.001

Zhang Jibin, Wu Pengxia, Hao Bo, et al. 2011. Heterotrophic nitrification and aerobic denitrification by the bacterium *Pseudomonas stutzeri* YZN-001. Bioresource Technology, 102(21): 9866–9869, doi: 10.1016/j.biortech.2011.07.118

Zhao Bin, An Qiang, He Yiliang, et al. 2012. N_2O and N_2 production during heterotrophic nitrification by *Alcaligenes faecalis* strain NR. Bioresource Technology, 116: 379–385, doi: 10.1016/j.biortech.2012.03.113

Zhao Bin, He Yiliang, Huang Jue, et al. 2010b. Heterotrophic nitrogen removal by *Providencia rettgeri* strain YL. Journal of Industrial Microbiology & Biotechnology, 37(6): 609–616

Zhao Bin, He Yiliang, Hughes J, et al. 2010a. Heterotrophic nitrogen removal by a newly isolated *Acinetobacter calcoaceticus* HNR. Bioresource Technology, 101(14): 5194–5200, doi: 10.1016/j.biortech.2010.02.043

Zhou Xiang, Xin Zhijun, Lu Xihong, et al. 2013. High efficiency degradation crude oil by a novel mutant irradiated from *Dietzia* strain by $^{12}C^{6+}$ heavy ion using response surface methodology. Bioresource Technology, 137: 386–393, doi: 10.1016/j.biortech.2013.03.097

Zhu Guibing, Peng Yongzhen, Li Baikun, et al. 2008. Biological removal of nitrogen from wastewater. In: Whitacre D M, ed. Reviews of Environmental Contamination and Toxicology. New York: Springer, 192: 159–195

Supplementary information:

Table S1. Subsystem feature counts of *Halomonas venusta* MA-ZP17-13

The supplementary information is available online at https://doi.org/10.1007/s13131-021-1897-9. The supplementary information is published as submitted, without typesetting or editing. The responsibility for scientific accuracy and content remains entirely with the authors.